Assessment of Landslide Volume for Alishan Highway Based On Database of Rainfall-Induced Slope Failure

Yun-Yao Chi, Ya-Fen Lee

Abstract—In this paper, a study of slope failures along the Alishan Highway is carried out. An innovative empirical model is developed based on 15-year records of rainfall-induced slope failures. The statistical models are intended for assessing the volume of landslide for slope failure along the Alishan Highway in the future. The rainfall data considered in the proposed models include the effective cumulative rainfall and the critical rainfall intensity. The effective cumulative rainfall is defined at the point when the curve of cumulative rainfall goes from steep to flat. Then, the rainfall thresholds of landslide are established for assessing the volume of landslide and issuing warning and/or closure for the Alishan Highway during a future extreme rainfall. Slope failures during Typhoon Saola in 2012 demonstrate that the new empirical model is effective and applicable to other cases with similar rainfall conditions.

Keywords—Slope failure, landslide, volume, model, rainfall thresholds.

I. INTRODUCTION

IN Taiwan, two-thirds of the total land area is in the hill area and other in the plains. Therefore, the hill areas have to be developed and utilized when the plains can no longer meet the demand of the population and the economic activities. Rapid development of the communities in the hill areas has increased the impact of landslides, in terms of loss of properties and lives, in these areas. Taiwan is located at the collided subduction zone of the Philippine Sea Plate and the Eurasian plate, which results in many folds and faults in the formed mountains. Taiwan is also located in the western North Pacific typhoon belt. Due to a number of reasons such as typhoons, storms, rainy season, weakness of ecological environmental, and hillside development, the landslides and debris flows often occur, which cause the blockage of roadways, isolation of the mountain areas, and loss of properties and lives.

The disaster prevention along roadways in the hills areas should first rely on warning and prevention. To enhance the landslide volume of the highway slope-failure assessments system, a variety of factors should be considered and their impacts should be studied. In Taiwan, considering that rainfall is one of the direct causes of slope failure in the hills areas, the rainfall is selected as the basis for the proposed models in this paper.

Here, the slopes along the most important access roadway

Yun-Yao Chi is with the Department of Land Management and Development, Chang Jung Christian University, Tainan, Taiwan (e-mail: yunyao@mail.cjcu.edu.tw).

Ya-Fen Lee is with the Department of Leisure Recreation and Travel Management, Toko University, Chiayi, Taiwan (e-mail: 2007LR03@ mail.toko.edu.tw).

from the plains to the mountain of Chiayi area, namely, the Alishan Highway (Tai-18), are examined. In this study, the empirical models of landslide volume are established based on a database of slope failures along Tai-18, caused by heavy rainfall, over a period of 15 years. The results provide the prediction formulas for calculating the landslide volume for hazard managing Tai-18.

II. REVIEWS

A. Relations between Slope Failure and Rainfall

Slope failure is triggered by both earthquake and rainfall in Taiwan. For the rainfall-induced slope failures, a threshold is defined as the rainfall beyond which slope failure can be triggered. The rainfall threshold models may be physical-based [1]-[4] or empirical-based. The empirical-based rainfall threshold model is usually established by taking the lower bound of the rainfall conditions, such as rainfall intensity [5]-[8], rainfall duration [9], [10], [8], cumulative rainfall [11], [12], or antecedent rainfall [13], [14] that can cause slope failure.

B. Exact Time of Slope Failure

Ikeya (1983) [15] pointed out in a torrential rain that caused sediment disasters, the typical relationship between rainfall duration and cumulative rainfall is like the one shown in Fig. 1. First, there is some light rain at the beginning of the rainfall period. Then, the rainfall intensity starts to increase more rapidly. After a continuous rapid rainfall period and cumulative rainfall, the sediment disasters occur when the rainfall intensity decreases and the gradient of the cumulative rainfall curve become smaller. The data of slope failures along the Alishan Highway were collected and summarized over the past 15 years by the Alishan Public Works Section of the Fifth District Maintenance Office, Directorate General of Highways, Ministry of Transportation and Communication, Taiwan. At each occurrence of slope failure, the staff of Public Works Section measured the avalanche size and took photos as records shortly after the slope failure and definitely before the site clean-up. These records, including location and the volume of slope failure, are generally very accurate except the exact time of occurrence. In this paper, the records of landslides and slope failure along the Alishan Highway between 1996 and 2010 caused by typhoon torrential rain are examined and analyzed.
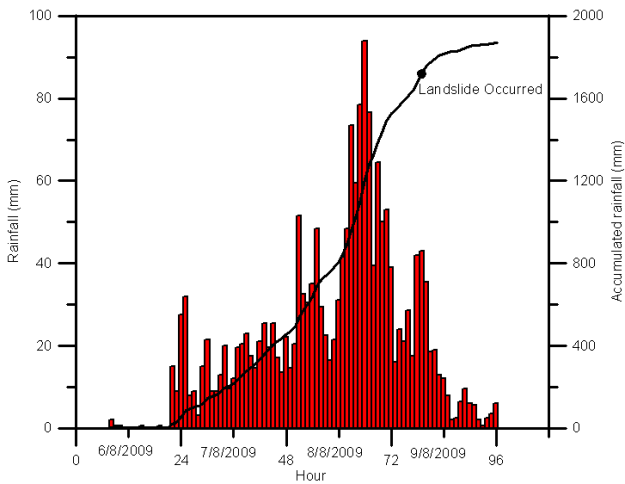
World Academy of Science, Engineering and Technology
International Journal of Environmental and Ecological Engineering
Vol:7, No:10, 2013

Fig. 1 A typical rainfall diagram of slope failure

C. Slump Volume of Slope Failure

The slump soil/rock volume of slope failure along road infers the hazard magnitude. A direct calculating method of landslide volume is product of area and average depth of landslide. The data should be collected by site investigation or Geology Information System. Nevertheless, high quality case histories of landslide depth are collected difficultly. The exponent function is used to present the relation between area ratio of landslide (ρ) and cumulative rainfall (R) as follows [16]-[18].

$$\rho = \frac{\Sigma a}{A} = \alpha \times (R - R_o)^n \qquad (1)$$

where R_o is cumulated a rainfall threshold. The value ranges about from 200mm to 400mm in site investigation in Taiwan [19]. Parameter "a" is indicated the area of slope failure, and the parameter "A" is total area of slope. In this paper, (1) is adapted to develop advanced for a relation function between landslide volume and rainfall characteristics.

III. STUDY CASES

The data of 18 rainfall events with highway slope failures and additional 71 rainfall events without slope failures are collected in this study. These rainfall event data include a histogram of rainfall per hour (rainfall intensity, I) and a cumulative rainfall curve. As shown in Table I, there were a total of 253 landslides caused by 18 typhoons with slope failures in the low altitude section of the Alishan Highway, with a total landslide volume of 150,418 m^3, which averages about 595 m^3/site. In the medium altitude section, there were 165 landslides with a total landslide volume of 119,753 m^3, which averages about 726 m^3/site. In the high altitude section, there were 106 landslides with a total landslide volume of 115,758 m^3, which averages about 1,092 m^3/site. In the Table I, the parameter "I_{max}" indicated the maximum value of rainfall intensity during histogram of rain.

IV. RESULTS

A. Distribution of Slope Failure

The total number of heavy rainfall of typhoon is 89 during 1996 to 2010 year in Taiwan. There are 18 typhoons that induced slope failures. The frequency diagram is showed as Fig. 2. The occurred duration of typhoon is from April to December. Although the slope failure occurred is during from July to October. The highest frequency of typhoon occurred in August is 26.97%. There two-thirds typhoons induced slope failure is occurred from July to August along the Alishan Highway in the past 15 years.
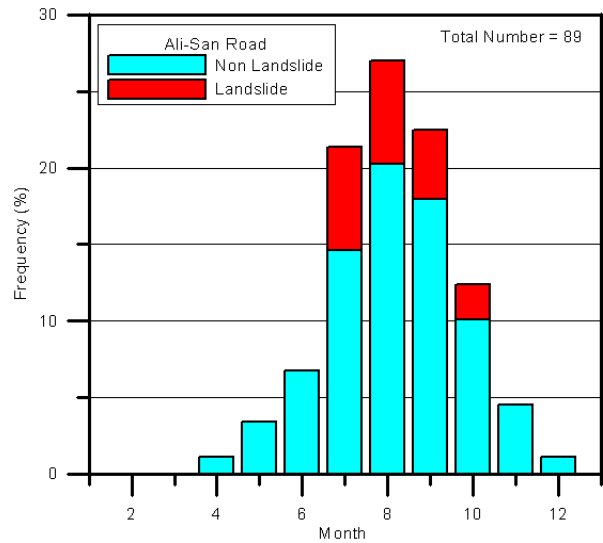

Fig. 2 The month distribution of slope failure along the Alishan Highway from 1996 to 2010 year

B. Landslide Volume Assessment Model

There are two parameter, the cumulative rainfall (R) and the characteristic rainfall intensity (CRI) are adapted to develop the landslide volume assessment models in this paper. The CRI is indicated as follows:

$$CRI = I_{max} + 2R/T \qquad (2)$$

where T is the duration of a rainfall in the unit of hour. The rainfall threshold value of R and CRI is determined by the highest successful ratio of discrimination for slope failure. The successful ratio is defined as follows:

$$p(X_o) = \frac{m_1 + m_2}{n} \times 100\% \qquad (3)$$

where m_1 is the number of which landslide volume is equal to zero in the cases of slope failure is not occurred in practical, m_2 is the number of which landslide volume is not equal to zero in the cases of slope failure is occurred in practical, n is the total number of cases.

There are two part of data is divided from the case histories

World Academy of Science, Engineering and Technology
International Journal of Environmental and Ecological Engineering
Vol:7, No:10, 2013

as Table I. They are named the low altitude section and the medium-high altitude section. Fig. 3 shows the relation curves of the two parts via the database. The formula of relation curve via cumulative rainfall (R) is defined as follows:

For the low altitude section：

$$V = \begin{cases} 0, & \text{when } R \leq 230 \text{ (mm)} \\ 1300 \times (R - 230)^{0.5}, & \text{otherwise} \end{cases} \quad (3)$$

For the medium-high altitude section：

$$V = \begin{cases} 0, & \text{when } R \leq 243 \text{ mm} \\ 1000 \times (R - 243)^{0.5}, & \text{otherwise} \end{cases} \quad (4)$$

The values of coefficient of determination for (3) and (4) are 0.52 and 0.37, respectively. The values of rainfall threshold are 230 mm and 243mm for the low and the medium-high altitude section, respectively. Although, two value are closer to each other.
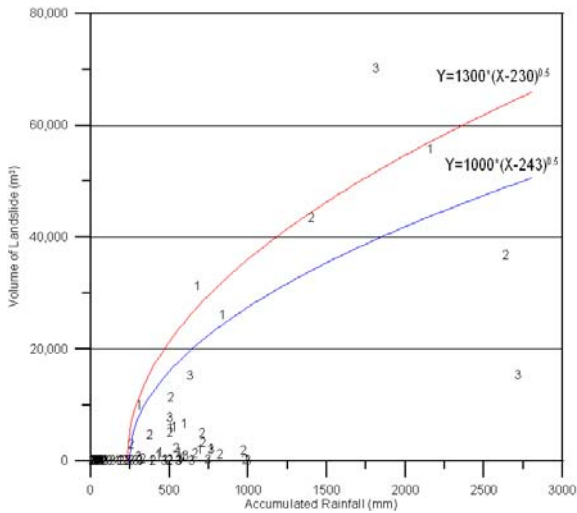

Fig. 3 The relation curves of the two parts via the cumulative rainfall (R) of the database. (Remark "1" = the low altitude section, "2" = the medium altitude section, and "3" = the high altitude section.)

Fig. 4 shows the relation curves of the two parts via the CRI of the database. The formula of relation curve via critical rainfall intensity (CRI) is defined as follows:

For the low altitude section：

$$V = \begin{cases} 0, & \text{when } CRI \leq 47 \text{ mm/hr} \\ 10 \times (CRI - 47)^{2}, & \text{otherwise} \end{cases} \quad (5)$$

For the medium-high altitude section：

$$V = \begin{cases} 0, & \text{when } CRI \leq 47 \text{ mm/hr} \\ 10 \times (CRI - 47)^{1.7}, & \text{otherwise} \end{cases} \quad (6)$$

The values of coefficient of determination for (5) and (6) are 0.58 and 0.55, respectively. The both values of rainfall

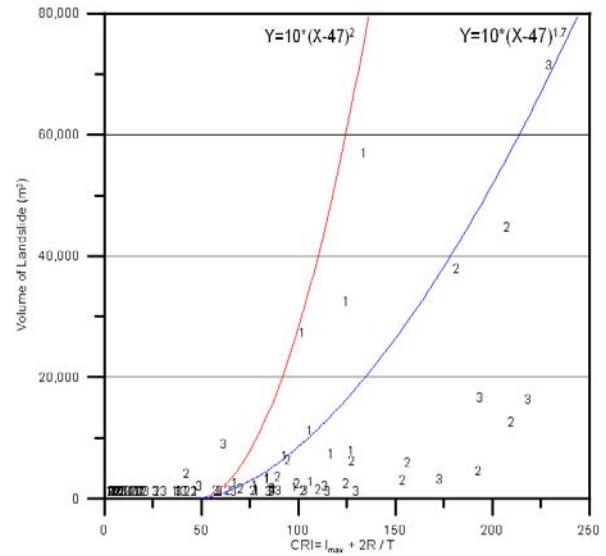threshold are 47 mm/hr for the low and the medium-high altitude section.

Fig. 4 The relation curves of the two parts via the critical rainfall intensity (CRI) of the database. (Remark "1" = the low altitude section, "2" = the medium altitude section, and "3" = the high altitude section.)

Table II shows the validation of the proposed model using slope failure data caused by the Saola typhoon in 2012 year in the Alisan Highway. The results of the cumulative rainfall based model ((3) and (4)) and the critical rainfall intensity based model ((5) and (6)) is compared. The error percentage of results for case 1 and case 2 (Table II) via the cumulative rainfall based model (in V_R column) and the critical rainfall intensity based model (in V_CRI column) is 27.7% and 47.5%, respectively. The result can be accepted for highway hazard management in practical.

V. CONCLUSION

In this paper we established an innovative empirical model, in which the landslide volume can be calculated based on effective cumulative rainfall (R) and critical rainfall intensity (CRI). The approach is demonstrated through a case study of the Alishan Highway, in which empirical model of landslide volume is established based on 15 years of typhoon-induced rainfall data and field observations of slope failures. The main results of this paper are summarized as follows:

1) The occurrence duration of typhoon is from April to December. Although the slope failure occurrence is from July to October. The highest frequency of typhoon occurrence in August is 26.97%. There two-thirds typhoons-induced slope failure occurrence is from July to August along the Alishan Highway in the past 15 years.

2) The values of accumulative rainfall threshold are 230mm and 243mm for the low and the medium-high altitude section, respectively. Although, two value are closer to each other.

3) The both values of critical rainfall threshold (CRI) are 47

World Academy of Science, Engineering and Technology
International Journal of Environmental and Ecological Engineering
Vol:7, No:10, 2013

mm/hr for both the low and the medium-high altitude section.

4) The empirical formula ((3) and (4)) of relation curve of landslide volume via cumulative rainfall (R) is developed. The values of coefficient of determination for the low altitude and medium-high altitude are 0.52 and 0.37,

respectively.

5) The empirical formula ((5) and (6)) of relation curve of landslide volume via critical rainfall intensity (CRI) is developed. The values of coefficient of determination for the low altitude and medium-high altitude are 0.58 and 0.55, respectively.

TABLE I
THE DATA LIST FOR THE CASE HISTORIES OF THE ALISHAN HIGHWAY

NO.	Year	Month	Elevation*	R (mm)	I_{max} (mm/hr)	T (hr)	No. of Landslide	Volume of landslide (m^3)
1	1996	5	1	24	3	24	0	0
2	1996	5	2	35.5	3.5	25	0	0
3	1996	5	3	62.5	7	24	0	0
4	1996	7	1	48.5	10	14	0	0
5	1996	7	2	40.5	10	9	0	0
6	1996	7	3	67	16	9	0	0
7	1996	8	1	836.5	48	31	33	26073
8	1996	8	2	1404	120	32	36	43456
9	1996	8	3	1816	112.5	31	21	70217
10	1996	9	1	10.5	1	16	0	0
11	1996	9	2	7.5	1.5	9	0	0
12	1996	9	3	13	3	9	0	0
13	1997	8	1	94	10.5	21	0	0
14	1997	8	1	168	25.5	26	0	0
15	1997	8	1	168	25.5	26	0	0
16	1997	8	2	215	22.5	21	0	0
17	1997	8	2	191.5	31	25	0	0
18	1997	8	2	191.5	31	25	0	0
19	1997	8	3	238.5	18	23	0	0
20	1997	8	3	242.5	40	25	0	0
21	1997	8	3	242.5	40	25	0	0
22	1998	8	2	374.5	94	12	8	4624
23	1998	8	3	318	72.5	15	0	0
24	1998	9	1	27	3.5	25	0	0
25	1998	9	2	32	4.5	23	0	0
26	1998	9	3	39.5	7	24	0	0
27	1998	10	1	186	24	30	0	0
28	1998	10	1	71.5	6.5	51	0	0
29	1998	10	2	309.5	42.5	29	1	150
30	1998	10	2	83.5	11	51	0	0
31	1998	10	3	306	28.5	30	1	801
32	1998	10	3	95.5	8	49	0	0
33	1999	6	1	23.5	8	29	0	0
34	1999	6	2	21.5	3.5	27	0	0
35	1999	6	3	41.5	7.5	31	0	0
36	1999	8	1	7.5	2.5	27	0	0
37	1999	8	2	11	3	27	0	0
38	1999	8	3	16.5	2.5	28	0	0
39	1999	10	1	26	4	18	0	0
40	1999	10	2	30	4	21	0	0
41	1999	10	3	57	6	29	0	0
42	2000	7	1	64.5	10.5	33	0	0
43	2000	7	2	78	15.5	34	0	0
44	2000	7	3	122.5	15	38	0	0
45	2000	8	1	229.5	27.5	24	0	0
46	2000	8	1	40.5	27.5	8	0	0
47	2000	8	2	256	22	25	3	2891
48	2000	8	2	65	19.5	17	0	0
49	2000	8	3	260	21	26	0	0
50	2000	8	3	47	12	16	0	0
51	2000	11	1	72	8	26	0	0
52	2000	11	2	87	9	29	0	0
53	2000	11	3	144	16	28	0	0
54	2001	7	1	306.5	65	15	14	9971
55	2001	7	2	509.5	137	14	15	11347
56	2001	7	3	634.5	121	13	26	15179
57	2001	9	1	675.5	70.5	25	32	31226
58	2001	9	2	502	66.5	23	1	188
59	2001	9	3	314	57.5	23	0	0
60	2004	7	1	504	52.5	25	19	5862
61	2004	7	2	504	52.5	24	9	5069
62	2004	7	3	568.5	53	34	11	474

World Academy of Science, Engineering and Technology
International Journal of Environmental and Ecological Engineering
Vol:7, No:10, 2013

63	2005	7	1	693.5	44	35	14	1948
64	2005	7	2	821	54	36	3	1205
65	2005	7	3	750	44	35	2	192
66	2005	8	1	593.5	80	25	22	6591
67	2005	8	2	663.5	71.5	25	12	1267
68	2005	8	3	602.5	65.5	25	6	815
69	2006	7	1	429.5	48	29	3	993
70	2006	7	2	501.5	43.5	30	1	45
71	2006	7	3	470	35.5	30	0	0
72	2007	8	1	439.5	38	30	10	1401
73	2007	8	2	397.5	33	30	1	11
74	2007	8	3	506	37	41	2	7700
75	2007	10	1	527	55	17	20	6088
76	2007	10	2	971	73	24	18	1835
77	2007	10	3	769	87.5	18	6	1966
78	2008	7	1	560	50.5	20	10	1446
79	2008	7	1	476	43	27	1	225
80	2008	7	2	713	121.5	20	10	3276
81	2008	7	2	545	50.5	28	2	2281
82	2008	7	3	562.5	76.5	21	1	30
83	2008	7	3	557	50	28	1	75
84	2008	9	1	764	53.5	50	7	2186
85	2008	9	1	589.5	54.5	27	8	681
86	2008	9	2	983	62.5	49	4	115
87	2008	9	2	710	75	27	6	4943
88	2008	9	3	1001.5	46.5	50	1	28
89	2008	9	3	643.5	64.5	33	1	75
90	2009	8	1	2155.5	75.5	74	60	55727
91	2009	8	2	2638.5	110.5	74	33	36719
92	2009	8	3	2719	123	77	26	15342
93	2010	9	1	383.5	55.5	33	0	0
94	2010	9	1	35	9	9	0	0
95	2010	9	1	33	9.5	14	0	0
96	2010	9	2	328.5	50.5	33	2	331
97	2010	9	2	29	5.5	9	0	0
98	2010	9	2	22.5	6	15	0	0
99	2010	9	3	286.5	38.5	30	1	92
100	2010	9	3	41.5	8	10	0	0
101	2010	9	3	21	5	13	0	0
102	2010	10	1	7.5	2	5	0	0
103	2010	10	2	7.5	2	6	0	0
104	2010	10	3	10	3.5	6	0	0

*Remark: "1" = the low altitude section, "2" = the medium altitude section, and "3" = the high altitude section.

TABLE II
VALIDATION OF THE PROPOSED MODEL USING SLOPE FAILURE DATA IN 2012 YEAR IN THE ALISHAN HIGHWAY

NO	Location	Date	ELE*	R(mm)	T(hr)	I_{max} (mm/hr)	CRI = I+2R/T	V_R (m³)	V_CRI (m³)
1	Alishan	2012/8/1	1	473.5	23	45	86.17	20285.8	15346.0
2	Alishan	2012/8/3	3	527	19	51	106.47	16852.3	10382.6

*Remark: "1" = the low altitude section, "2" = the medium altitude section, and "3" = the high altitude section.

REFERENCES

[1] P. D'Odorico, S. Fagherazzi," A probabilistic model of rainfall-triggered shallow landslides in hollows: a long-term analysis." (ESG 6–1) Water Resources Research 39, 6-14, 2003.
[2] A.S.Muntohar, H.J. Liao," Analysis of rainfall-induced infinite slope failure during typhoon using a hydrological–geotechnical model." Environmental Geology 56, 1145–1159, 2009.
[3] C.C. Huang, S.C. Yuin, "Experimental investigation of rainfall criteria for shallow slope failures," Geomorphology 120, 326–338, 2010.
[4] M, Safaei, H. Omar, B.K. Huat, Z.B.M. Yousof, V. Ghiasi," Deterministic rainfall induced landslide approaches, advantage and limitation. (16 Bund. U), "Electronic Journal of Geotechnical Engineering 1619–1650, 2011.
[5] F. Guzzetti, S. Peruccacci, M. Rossi, and C.P. Stark, "Rainfall thresholds for the initiation of landslides in central and southern Europe," Meteorology and atmospheric physics, vol. 98, no. 1-2, pp. 239-267, 2007.
[6] R.L. Dahal, S. Hasegawa,". Representative rainfall thresholds for landslides in the Nepal Himalaya. Geomorphology 100, 429–443, 2008.
[7] P. Jaiswal, C.J.V Westen, ". Estimating temporal probability for landslide initiation along transportation routes based on rainfall thresholds". Geomorphology 112, 96–105, 2009.
[8] H. Saito, D. Nakayama, H. Matsuyama, "Relationship between the initiation of a shallow landslide and rainfall intensity-duration thresholds in Japan." Geomorphology 118, 167–175, 2010.
[9] M. Floris, F. Bozzano, ". Evaluation of landslide reactivation: a modified rainfall threshold model based on historical records of rainfall and landslides." Geomorphology 94, 40–57, 2008.
[10] M.T. Brunetti, S. Peruccacci, M. Rossi, S. Luciani, D. Valigi,F. Guzzetti, " Rainfall thresholds for the possible occurrence of landslides in Italy. " Natural Hazards and Earth System Sciences 10, 447–458, 2010.
[11] M. Floris, F. Bozzano, "Evaluation of landslide reactivation: a modified rainfall threshold model based on historical records of rainfall and landslides. " Geomorphology 94, 40–57, 2008.

[12] C. Li, T. Ma, X. Zhu, W. Li," The power–law relationship between landslide occurrence and rainfall level." *Geomorphology* 130, 221–229, 2011.

[13] T. Glade, M. Crozier, P. Smith," Applying probability determination to refine landslide-triggering rainfall thresholds using an empirical "antecedent daily rainfall model". *Pure and Applied Geophysics* 157, 1059–1079, 2000.

[14] P. Jaiswal,, C.J.V. Westen, " Estimating temporal probability for landslide initiation along transportation routes based on rainfall thresholds. *Geomorphology* 112, 96–105, 2009.

[15] H. Ikeya, *Methods of Debris Flow Forecast*, Kajima Institute publishing Co. Ltd, Japan, pp. 65–70, 1983.

[16] T. Uchihugi, "Landslides due to one continual rainfall," *JSECE*, 23(4), pp 79, 1971.

[17] S.C. Chen, Y.Z. Tasi, C.H. Wu," Distinguishing landslide morphology and landslide volume estimate in Siaolun village," *Journal of Engineering Environment*, No.25, 45-56, 2010.

[18] B.S. Lin, W.Y. Leung, S.Y. Chi, W.C. Lo," Applying GIS and Remote Sensing to Simply Estimate Landslide Volume of Typhoon Events in a Watershed," *2011 International Conference on Fuzzy Systems and Neural Computing*, 136-139, 2011.

[19] Y.Y. Chi, *Risk Assessment of Natural Disaster*. Taiwan: Tsang Hai Book Publishing Co., 2011.